JOC The Journal of Organic Chemistry

Featured Article

pubs.acs.org/joc

Left-Handed Helical Preference in an Achiral Peptide Chain Is Induced by an L-Amino Acid in an N-Terminal Type II β-Turn

Matteo De Poli,[†] Marta De Zotti,[‡] James Raftery,[†] Juan A. Aguilar,[†] Gareth A. Morris,[†] and Jonathan Clayden*[,†]

[†]School of Chemistry, University of Manchester, Oxford Road, Manchester M13 9PL, U.K.

[‡]Dipartimento di Scienze Chimiche, Università di Padova, via Marzolo 1, 35131 Padova, Italy

Supporting Information

ABSTRACT: Oligomers of the achiral amino acid Aib adopt helical conformations in which the screw-sense may be controlled by a single N-terminal residue. Using crystallographic and NMR techniques, we show that the left- or right-handed sense of helical induction arises from the nature of the β-turn at the N terminus: the tertiary amino acid L-Val induces a left-handed type II β-turn in both the solid state and in solution, while the corresponding quaternary amino acid L-α-methylvaline induces a right-handed type III β-turn.

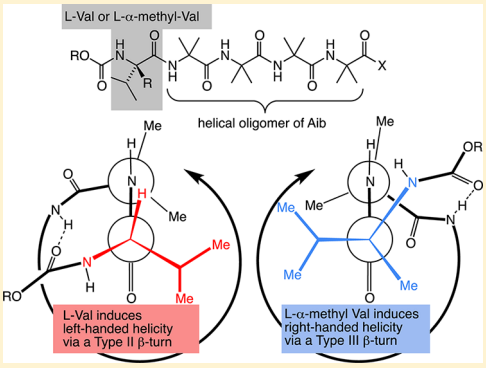

INTRODUCTION

Oligomers of the achiral quaternary α-amino acid Aib (2-aminoisobutyric acid) adopt helical conformations in which each monomer is hydrogen bonded to the monomer three positions further along the chain (Figure 1).[1−4] The stability of this conformation, known as a 3_{10}-helix,[5] over the more typical peptide α-helix is a result of the "conformational Thorpe−Ingold effect":[6] the geminally dimethylated quaternary carbon atom of the monomer favors more tightly twisted chain conformations.

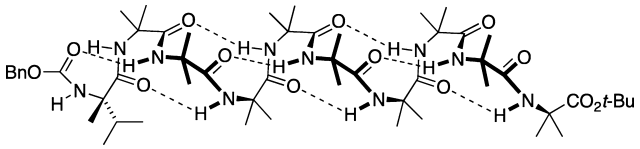

Figure 1. Right-handed 3_{10} helical conformation of an Aib_9 oligomer capped by an N-terminal Cbz-L-α-methylvaline [L-(αMe)Val] residue.[10]

Because Aib is achiral, 3_{10}-helices containing only Aib display no preference for left- or right-handed screw-sense, and indeed Aib oligomers undergo conformational inversion on a time scale of milliseconds or less.[7−9] However, we,[10] and others,[11] have shown that this dynamic equilibrium may be biased in favor of either the left- or right-handed screw-sense by incorporating a chiral residue at the chain terminus[10] or by noncovalent interaction with chiral ligands.[11] We developed a simple NMR method to report on the degree of control obtained:[12] for example, an N-terminal Cbz-L-valine induces a 65:35 screw-sense preference while an N-terminal Cbz-L-α-methylvaline [L-(αMe)Val] induces a 76:24 screw-sense preference in the oligomer shown in Figure 1.

During this work, it was evident that the preferred screw-sense induced in the helix depended not only on the configuration of the chiral N-terminal residue but also on whether it was tertiary (as in the "normal" proteinogenic amino acids L-Phe and L-Val) or quaternary (for example, L-α-methylvaline or L-isovaline [L-Iva]).[13] L-Val and L-Phe induce left-handed helicity in an oligo-Aib helix, while L-(αMe)Val or L-Iva induce right-handed helicity. This seemed all the more remarkable, given that peptide helices made of C^{α}-trisubstituted L-amino acids are typically right handed.[14,15]

The hydrogen-bonding pattern in a 3_{10}-helix matches that in a peptide β-turn. According to the definition of Venkatachalam,[16] these are regions involving four consecutive amino acid residues where the polypeptide chain folds back on itself by nearly 180°, classified as type I, II, and III (Figure 2).

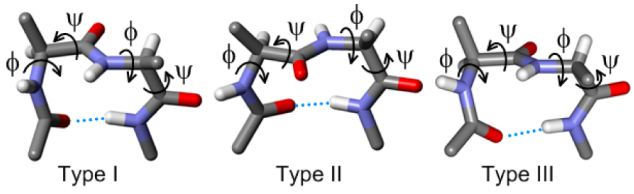

Figure 2. Three ideal types of β-turns.

Received: December 13, 2012
Published: January 14, 2013

Specifically, they differ in the conformation of the chain held by a hydrogen bond between C═O of residue i and NH of residue $i + 3$, which is described by φ, ψ torsion angles of $(i + 1)$ and $(i + 2)$ residues of the turn (Table 1). An extended 3_{10}-helix is in essence a stack of type III β-turns (Figure 2).

Table 1. Torsion Angle Values (deg) for Three Major Types of β-Turn

β-turn	φ $(i + 1)$	ψ $(i + 1)$	φ $(i + 2)$	ψ $(i + 2)$
type I	−60	−30	−90	0
type II	−60	+120	+80	0
type III	−60	−30	−60	−30

Of these three conformations, it is worth noting that the sense of twist in type II and type III β-turns is opposite because two torsion angles are of opposite sign. It is reasonable to infer that the opposite screw sense induced by tertiary and quaternary amino acids is due to their differing preferences for type II vs type III β-turn conformations[17] and that this difference leads to opposite senses of twist that are propagated into the remainder of the oligo-Aib helix through the hydrogen-bonding network.[2,17,18]

In this paper, we present the experimental evidence that this is indeed the case. Studies were carried out on four helical peptides **1**−**4**.

Peptide **1**: Ac-L-Val-Aib$_4$-Gly-NH$_2$
Peptide **2**: Ac-L-(αMe)Val-Aib$_4$-Gly-NH$_2$
Peptide **3**: Ac-L-Val-Aib$_4$-O-*t*-Bu
Peptide **4**: Ac-L-(αMe)Val-Aib$_4$-OH

RESULTS

1. Conformational Analysis in the Crystalline State. The first experimental evidence for the correlation between peptide helix screw sense and different types of turns at their N-termini was obtained by means of X-ray diffraction analysis. Peptides **1** and **2** did not crystallize under any of the conditions tried, but the closely related peptides Ac-L-Val-Aib$_4$-O*t*-Bu **3** and Ac-L-(αMe)Val-Aib$_4$-OH **4**, which differ from **1** and **2** only in the C-terminal residue, have crystals suitable for single-crystal X-ray diffraction studies. Their X-ray crystal structures are shown in Figures 3 and 4. Crystal data and structure refinements are reported in Table S1 (Supporting Information). Backbone (ϕ, ψ) torsion angles and intramolecular H-bond distances are reported in Table 2.

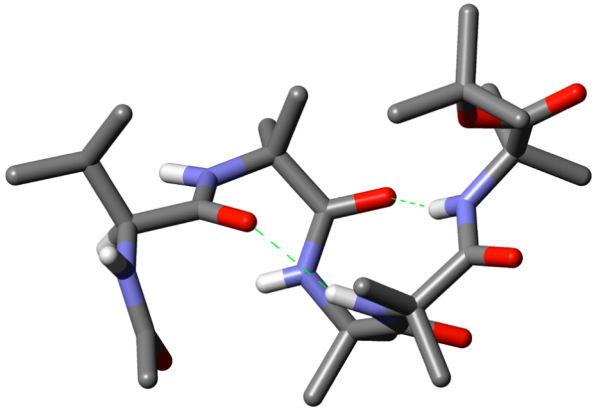

Figure 3. X-ray crystal structure of Ac-L-Val-Aib$_4$-O-*t*-Bu (**3**).

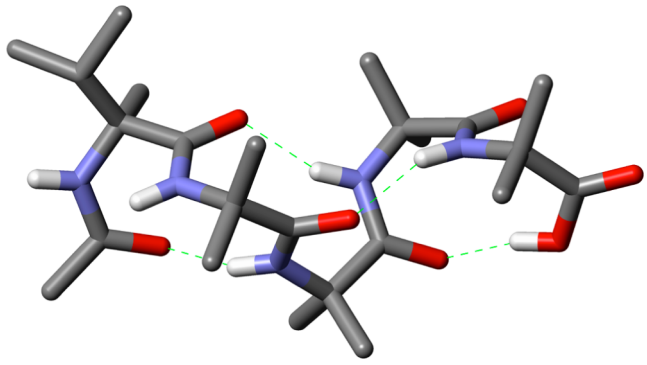

Figure 4. X-ray crystal structure of Ac-L-(αMe)Val-Aib$_4$-OH (**4**).

Inspection of (ϕ, ψ) backbone torsion angles in Table 2 reveals that they belong to the $3_{10}/\alpha$-region of the Ramachandran plot[19,20] and confirms the strong folding propensities of Aib-rich short peptides. Both compounds form mainly 3_{10}-helical structures in the body of their $(Aib)_n$ chains, stabilized by consecutive intramolecular 1←4 C═O···H−N bonds (type III β-turns).[16] The mean backbone (ϕ, ψ) values of peptide **3** and **4** are (56°, 30°) and (−51°,−37°), respectively, very close to the published average values (−57°,−30°).

Interestingly, the (ϕ, ψ) values in the two peptides are of similar magnitude but of opposite sign, reflecting the reversed screw sense observed in the two structures (apart from ϕ of Val[1] in peptide **3** which retains a negative value as expected for L amino acids[21]). In particular, sign inversion takes place at ψ of Val[1] of peptide **3** (see Table 2) which corresponds to position $i + 2$ of the first helix β-turn.[16] This fact accounts for the presence of a distorted β-turn of type II at the peptide N-terminus, which propagates a left-handed screw sense through the rest of the Aib chain.

When L-(αMe)Val is at peptide N-terminus (peptide **4**) the structure folds into a well-developed series of type III β-turns, maintained until the last C-terminal residue where a hydrogen bond is detected between COOH of Aib[5] and C═O of Aib[3].[22] The C-terminal Aib[5] residue of peptide **3**, on the other hand, shows a reversal of the helix screw sense (negative ϕ, ψ values) resulting from the presence of the C-terminal ester (and unrelated to the N-terminal structure). This conformational feature relieves the unfavorable O···O interaction taking place between the C═O of Aib[3] and either oxygen atom of the ester functionality of C-terminal Aib[5] residue, by rotating its ϕ torsion by 180°.[23,24]

2. Conformational Analysis in Solution. We have previously used[13] circular dichroism (CD) to show that the principal conformations of peptides **1** and **2** in methanol are helices with opposite screw-senses, and time-dependent DFT calculations allowed us to correlate the CD spectrum of **1** with a left-handed helix and the CD spectrum of **2** with a right-handed helix. However, CD did not reveal sufficiently detailed information for us to draw conclusions about the structure of the N-termini of peptides **1** and **2** in solution. We therefore carried out a detailed investigation using NMR spectroscopy. Experiments were carried out in CD_3OH in order to preserve amide NH proton signals, allowing their identification, and to allow us to compare our findings with those previously obtained by CD under the same experimental conditions.

To detect the proposed N-terminal type-II β-turn in peptide **1**, two independent NMR methods were used: first, interproton

dx.doi.org/10.1021/jo302705k | J. Org. Chem. 2013, 78, 2248−2255

Table 2. Structural Parameters for Ac-L-Val-Aib$_4$-O-*t*-Bu (3) and Ac-L-(αMe)Val-Aib$_4$-OH (4)

	3		4		$i-1$ C=O to $i+2$H–N H-bonding distance (Å)	
residue	ϕ (deg)	ψ (deg)	ϕ (deg)	ψ (deg)	3	4
Val[1] or (αMe)Val[1]	−69.0	166.4	−50.0	−43.2		
Aib[2]	57.3	27.6	−51.6	−37.0		2.11
Aib[3]	46.3	43.8	−54.8	−30.6	2.27	2.21
Aib[4]	65.1	19.9	−50.7	−30.2	2.11	2.14
Aib[5]	−33.9	−179.6	−48.5	−41.9		1.95[a]

[a]Hydrogen bond detected between residue Aib[3](C=O) and Aib[5](COOH).

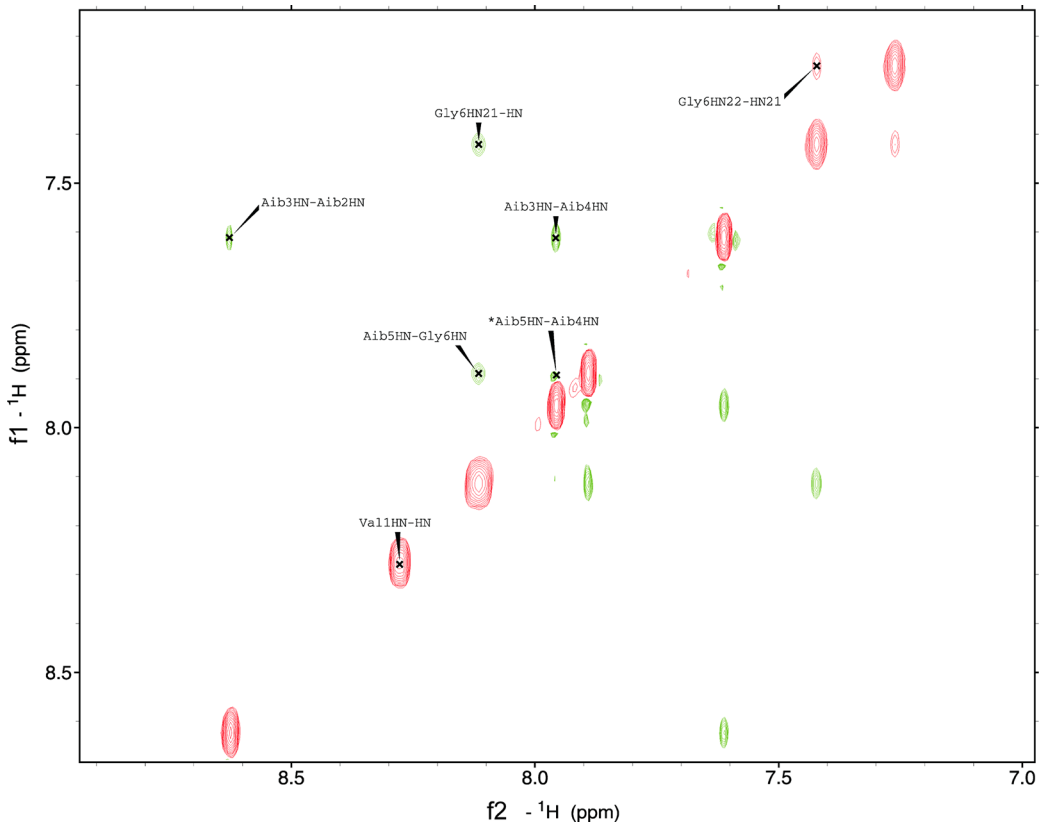

Figure 5. Amide region of the NOESY spectrum (500 MHz, τ_m = 280 ms) of peptide 1 (15 mM in MeOH-d_3; 298 K). *: sequential cross-peak overlapped by diagonal peaks. Gly6 HN21 and HN22: C-terminal amide protons.

distances estimated using NOE spectroscopy were compared with those found both in calculated structures and in the N-terminal segment of the X-ray crystal structure of the related peptide **3**, and second experimental coupling constants were used to calculate dihedral angles using the Karplus equation.

Overall assignment of proton and carbon signals for both peptides **1** and **2** was achieved using the standard procedure described by Wüthrich[25] (Tables S2 and S3, Supporting Information). The spin systems of the Val and Gly residues were identified using DQF-COSY and TOCSY spectra,[26,27] while HMQC[28] and HMBC[29] experiments were used to assign the Aib and (αMe)Val residues.

The ^{13}C atoms of the two methyl groups (indicated in Tables S1 and S2, Supporting Information, as β and β') of each Aib residue were found to resonate at different chemical shifts, above and below 25 ppm. Jung et al.[30] have shown that the anisochronicity of the ^{13}C NMR signals of a pair of diastereotopic methyl groups may be used as a marker of helix stability in solution. Typically, in the absence of higher order structures, the ^{13}C NMR signals of a *gem*-dimethyl group, even directly adjacent to a stereogenic center, are separated by less than 0.5 ppm. However, within a stable helical conformation, the anisochronicity (also known as "chemical nonequivalence" or CNE[30]) of the ^{13}C NMR signals of a *gem*-dimethyl group may exceed 2 ppm. Tables S4 and S5 (see the Supporting Information) report the anisochronicities in the ^{13}C NMR spectrum of the methyl groups of the four Aib residues of peptides **1** and **2**. Despite the short length of both peptides, all anisochronicities were found to be around 2 ppm, confirming the adoption of a stable helical conformation in MeOH solution. Stereospecific assignment of the two diastereotopic methyl groups in each Aib residue was achieved by means of HMQC spectra. As reported in the literature, each Aib residue of a peptide chain shows two distinct ^{13}C chemical shifts, one above and one below 25 ppm. This general behavior of Aib residues in polypeptides is a consequence of the different shielding tensors experienced by the pro-*R* (located in the

dx.doi.org/10.1021/jo302705k | J. Org. Chem. 2013, 78, 2248−2255

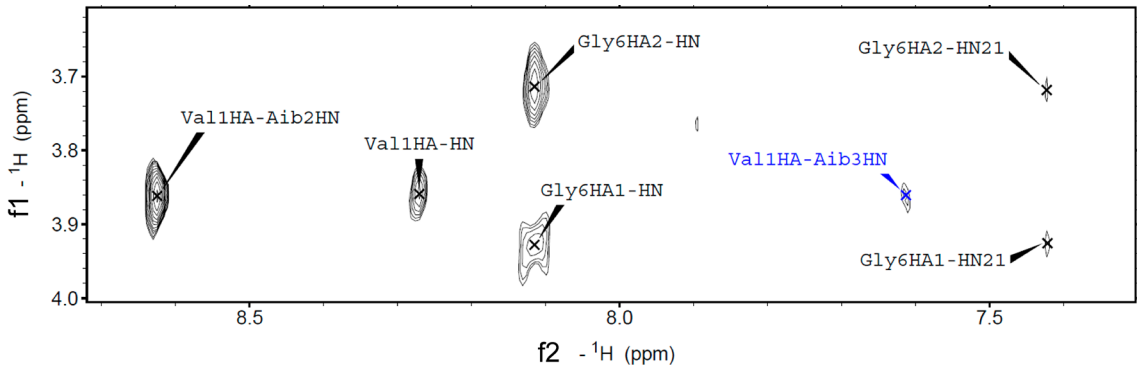

Figure 6. Fingerprint region of the NOESY spectrum (500 MHz, τ_m = 280 ms) of peptide **1** (15 mM in MeOH-d_3; 298 K). Medium-range ($i \rightarrow i + 2$) interaction is marked in color. Gly6 HN21: C-terminal amide proton.

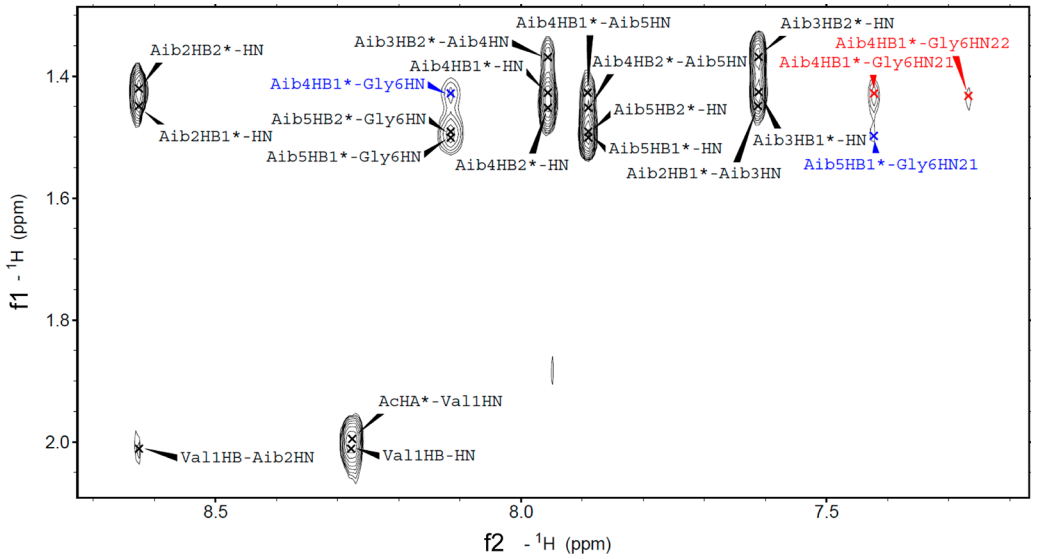

Figure 7. Region of the NOESY spectrum (500 MHz, τ_m = 280 ms) of peptide 1 (15 mM in MeOH-d_3; 298 K). Medium-range ($i \rightarrow i + 2$), diagnostic of the presence of a 3_{10}-helical structure, and ($i \rightarrow i + 3$) interactions are marked in blue and red, respectively. Gly6 HN21 and HN22: C-terminal amide protons.

position of the $^{\alpha}$H in a trisubstituted residue) and pro-*S* methyl groups.[31,32]

The sequential assignments for peptides **1** and **2** were obtained from HMBC and NOESY spectra.[27,33] To avoid spin diffusion, the build-up curve of NOE cross-peak intensities was first determined as a function of mixing time (τ_m = 50−500 ms). The optimal mixing time τ_m, balancing cross-peak intensity against relayed magnetization transfer, was found to be 280 ms for both the peptides. Relevant regions of the NOESY spectrum of peptide **1** are shown in Figures 5−7, while the amide region of the NOESY spectrum of peptide **2** is reported in Figure 8.

In the portions of the NOESY spectrum of peptide **1** shown in Figures 5 and 6, a strong cross-peak can be detected between Val^{1}C$^{\alpha}$H and Aib^{2}NH, while the intraresidue Val^{1}C$^{\alpha}$H−NH correlation peak has a much lower intensity and the Val^{1}NH−Aib^{2}NH cross-peak is hardly visible. This fact alone immediately suggests the presence of a type II β-turn at the peptide N-terminus, this being the only possible conformation where the Val^{1}C$^{\alpha}$H and Aib^{2}NH protons are in close spatial proximity.[17] All other expected diagnostic C$^{\alpha(\beta)}$H(i)−NH(i+3), C$^{\alpha(\beta)}$H(i)−NH(i+2) and sequential NH−NH cross peaks are visible (apart from those obscured by diagonal peaks) and

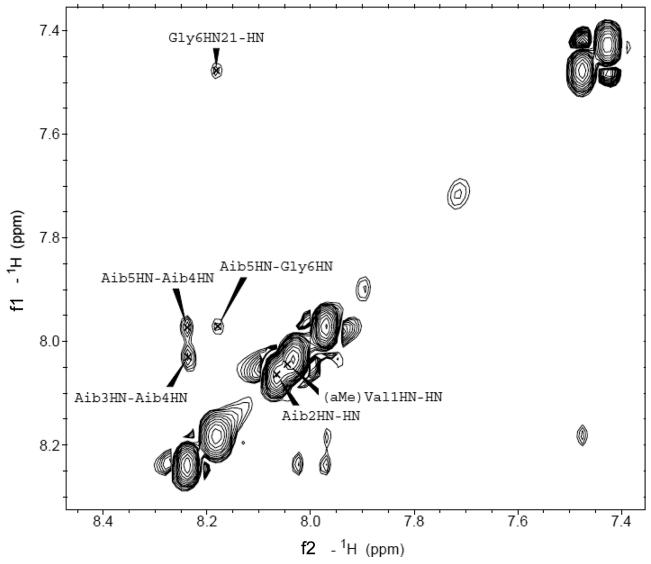

Figure 8. Amide region of the NOESY spectrum (500 MHz, τ_m = 280 ms) of peptide **2** (15 mM in MeOH-d_3; 308 K). Gly6 HN21: C-terminal amide proton.

dx.doi.org/10.1021/jo302705k | J. Org. Chem. 2013, 78, 2248−2255

confirm the presence of a mainly 3_{10}-helical structure throughout the rest of the sequence. Thus the presence of a different type of turn at the peptide N-terminus does not appear to affect the conformation of the rest of chain.

All the nonoverlapping cross-peaks detected in the NOESY spectrum of peptide **1** were integrated and the values used to estimate interproton distances as described in the Experimental Section. The most relevant NMR-derived distances are reported (with their standard deviations) in Table 3, along with the corresponding values obtained from the calculated model and the N-terminal portion of the X-ray crystal structure of peptide **3**. There is a good fit between the three sets of distances, justifying our interpretation of the NOE cross peaks associated with the Val[1] residue. In particular, all the distances involving the Ac-Val[1]-Aib[2] sequence are consistent with the presence of a type II β-turn and exclude the possibility of a type III β-turn.

Table 3. Distances (Å) Obtained by 2D-NMR, X-ray, and Calculated Model Structures for Peptide 1

distances	2D-NMR	X-ray	calculation
Val[1] H^{α}–HN	2.9 ± 0.3	2.80	2.87
Val[1] H^{α}–Aib[2] HN	2.2 ± 0.2	2.39	2.13
Val[1] H^{α}–Aib[3] HN^{a}	3.6 ± 0.4	3.59	3.77
Val[1] H^{α}–Aib[4] HN^{a}	*b*	4.74	5.07
Val[1] H^{α}–Aib[5] HN^{a}	*b*		7.24
Val[1] H^{α}–Aib[4] βH^{a}	*b*	6.12	6.64
Val[1] Ac–Aib[2] HN	*b*	6.01	5.14
Val[1] Ac–Aib[3] HN^{a}	*b*	5.45	4.08
Val[1] Ac–Aib[4] HN^{a}	*b*	4.58	4.96
Val[1] HN–Aib[2] HN	4.4 ± 0.4	4.64	4.46
Aib[2] HN–Aib[3] HN	2.9 ± 0.3	2.91	2.72
Aib[3] HN–Aib[4] HN	2.8 ± 0.3	2.83	2.79
Aib[5] HN–Gly[6] HN	2.8 ± 0.3		2.76
Gly[6] HN–$CONH_2$	2.8 ± 0.3		2.62

[a]Correlations that, if present, account for the presence of a helical conformation. [b]Not detected in the NOESY spectrum.

The existence of a type II β-turn at the N-terminus of peptide **1** was further supported by analysis of the dihedral angles obtained from coupling constants (Table 4). $^{1}J_{C\alpha H\alpha}$ and $^{3}J_{NH\alpha}$ of Val[1] were measured using nondecoupled HMQC[29] and phase-sensitive DQF-COSY.[34] Values of 141.1 Hz for $^{1}J_{C\alpha H\alpha}$ and 5.4 Hz for $^{3}J_{NH\alpha}$ were found. Both values deviate from those in residues embedded into a helical structure and are closer to those expected for either a random coil or a polyproline-type II structure.[35,36]

Table 4. Comparison between Observed and Characteristic Coupling Constants in Different Protein Secondary Structures[36]

constants	found	α-helical	random coil	poly-(Pro) II
$^{3}J_{HN\alpha}$	5.4	4.8	7.5	6.5
$^{1}J_{C\alpha H\alpha}$	141.1	146.3	141.5	142.6

The $^{3}J_{NH\alpha}$ coupling constant is related to the torsion angle ϕ by the Karplus eq 1:[37]

$$^{3}J_{NH\alpha} = 6.4\cos^{2}\theta - 1.4\cos\theta + 1.9 \quad (\text{where } \theta = |\phi - 60°|) \qquad (1)$$

For J = 5.4 Hz, and taking into account the allowed (ϕ, ψ) torsion angle regions[38] of the Ramachandran plot for L-Val, the dihedral angle ϕ was calculated to be −70°. Consequently, this value was used to determine ψ dihedral angles by means of eq 2:[35]

$$^{1}J_{C\alpha H\alpha} = 140.3 + 1.4\sin(\psi + 138°) - 4.1\cos 2(\psi + 138°) + 2.0\cos 2(\phi + 30°) \qquad (2)$$

The calculated ψ torsion angles falling into the allowed regions[38] of the Ramachandran plot for L-Val are ψ = 106° and ψ = 160°, both positive values. This observation explains why the N-terminal β-turn gives rise to a left-handed screw-sense in peptide **1**. Furthermore, as shown in Figure 9, the angles (ϕ, ψ = −69.0°, +166.4°) observed at Val[1] in the X-ray structure of peptide **3** fit nicely with one of the two possible pairs of (ϕ, ψ) values obtained by combining eqs 1 and 2, specifically (ϕ, ψ) = (−70°, +160°). This finding further proves that the N-terminal segment of peptide 1 is folded into a type II β-turn.

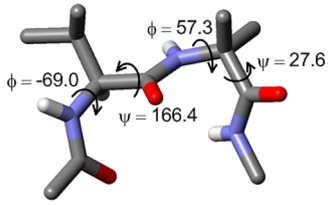

Figure 9. First turn (ϕ, ψ) torsion angles as observed in the X-ray crystal structure of peptide **3** (the rest of the molecule is omitted for clarity).

In regard to peptide **2**, the analysis was complicated by extensive overlapping in both the NH–NH and in the $^{\beta}CH_3$–NH proton correlation regions (Figure 8). To overcome this problem a range of temperatures was screened. The variation of the NMR spectrum with temperature is consistent with the presence of highly populated 3_{10}-helical structures. Indeed, as shown in Figure S1 and Table S6 (Supporting Information), the temperature dependence of NH chemical shifts in CD_3OH solution groups the NH protons into two distinct types: the two N-terminal NH protons exhibit significantly larger temperature coefficients (9 ppb/°C) than all other NH protons (between 4 and 3 ppb/°C).[39,40] Finally, the behavior of the two C-terminal amide protons suggests that one is intramolecularly hydrogen bonded while the other is not.

Some of the diagnostic peaks indicating a 3_{10}-helical conformation were visible in the NOESY spectrum of peptide **2**, although signal overlapping prevented us performing an in-depth analysis of the 2D NMR data, as done for peptide **1**. Furthermore, the strong helicogenic propensities of L-(αMe)-Val are well-known.[41,42] When embedded into a peptide sequence, this residue folds preferentially into right-handed 3_{10}-helices, as seen in the X-ray crystal structure of peptide **4** (Figure 4). It is safe to conclude therefore that peptide 2 adopts a well developed, right-handed 3_{10}-helical conformation in solution similar to the one observed in the solid state.

DISCUSSION

This work indicates that the role of proteinogenic, tertiary amino acids (such as valine) in controlling the handedness of Aib helices is dependent on their position in the sequence. L-Val in a nonterminal position induces right handed helicity in

dx.doi.org/10.1021/jo302705k | J. Org. Chem. 2013, 78, 2248–2255

an Aib tetramer,[23] and L-amino acids in general participate in right-handed helical structures.[14] Related studies have been carried out on achiral peptides containing dehydroamino acids.[17,43,44] Furthermore, amino acids possessing a β-branched, hydrophobic side chain (such as Val or Ile) are known to destabilize helical structures[45,46] while favoring β-sheet formation.[47,48]

The effect on the N-terminal turn of the relatively small difference between the L-Val and L-(αMe)Val residue can be analyzed by viewing the first turn of each helix in the form of a Newman projection (Figure 10). A type II turn with a tertiary

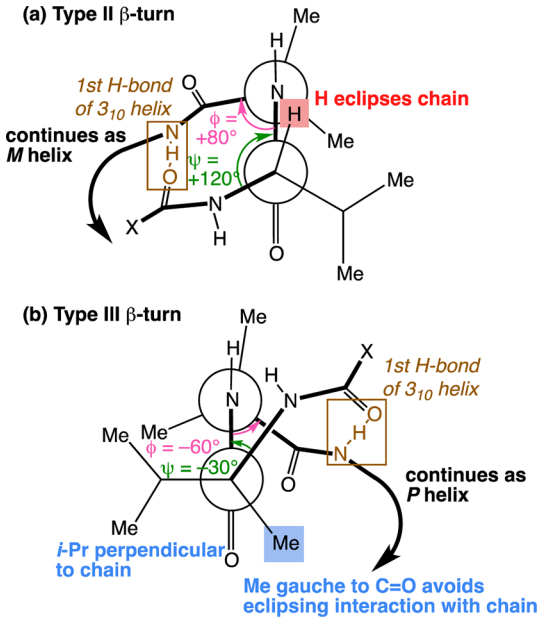

Figure 10. Newman projections of the N-terminal turns of (a) L-Val and (b) L-(αMe)Val capped helices. For acetyl, X = Me.

L-amino acid at position i + 1 allows the amino acid side chain (an isopropyl group in the case of L-Val) to adopt an unhindered position gauche to the carbonyl group of the same residue (Figure 10a). The acylated amino group is poised to hydrogen bond with the NH group of residue i + 3 without incurring unfavorable eclipsing interactions, since only the C^{α}–H bond need eclipse the chain (specifically, the C–N bond of the amide linkage between i + 1 and i + 2). This hydrogen bond leads to a left-handed (M) helix.

On exchanging the L-tertiary amino acid for an L-quaternary amino acid, the C^{α}–H bond must be replaced by a C–C bond, resulting in an eclipsing interaction. The result is a destabilization of the type II β-turn, and the adoption instead of a type III β-turn (Figure 10b). In this structure, one of the two C^{α} substituents (preferably the more hindered group; isopropyl in the case of L-(αMe)Val) is perpendicular to the C=O group, while the other finds itself gauche to the C=O group. Hydrogen bonding between the C=O of the acylated amino group and the NH of residue i + 3 again continues a helix, but this time a right-handed (P) one.

These conformations represent only the most stable of those possible: we know that the left- or right-handed screw-sense preference induced by both L-Val and L-(αMe)Val is only of the order of 3:1,[12] so other conformations must also be adopted to a lesser extent, populating the less favorable screw-sense. For L-(αMe)Val, these might conceivably include a type III′ β-turn, i.e., a type III structure with a left-handed twist in which the Me and i-Pr groups have changed places. However, it seems unlikely that an N-terminal L-Val will adopt a type II′ β-turn, in which there would be a severe eclipsing interaction. Therefore, it may be that the type III β-turn is also populated by the L-Val-capped peptide **1** to a lesser extent.[49]

Analogous behavior by other N-terminal tertiary amino acids in the solution phase is supported by both our conformational analysis of **1** and **3** and CD spectra of similar Aib-rich peptides.[13] Furthermore, this conformational feature arises regardless of the identity of the N-terminal amino acid side chain or protecting group, as shown by the common screw-sense also observed in phenylalanine and alanine capped peptides.[13] It seems reasonable therefore to conclude that the left-handed screw sense (M helicity) exhibited by these Aib-rich peptides is the result of an N-terminal type II β-turn conformation.[50]

CONCLUSION

Previous work[13] has shown, by using circular dichroism spectroscopy and time-dependent DFT calculations, that L-valine induces a left-handed screw-sense when attached to the N-terminus of an Aib oligomer, while its quaternary analogue L-α-methylvaline induces a right-handed screw sense. X-ray crystallography of two representative Aib oligomers suggests that the origin of the difference lies in the contrasting β-turn conformations adopted at the N-terminus of the helix. The detailed NMR investigations presented here support this view, and we conclude that in solution tertiary L-amino acids (of which L-valine is representative) at the N-terminus of an Aib oligomer induce left handed helicity by promotion of a Type II β -turn, while quaternary L-amino acids (of which L-α-methylvaline is representative) conversely induce right-handed helicity by promotion of a Type III β-turn.

EXPERIMENTAL SECTION

Synthesis. The synthesis of peptides **1** and **2** has been published.[13]

*Ac-Val-Aib$_4$-Ot-Bu (**3**).* Cbz-L-Val-Aib$_4$-O-*t*-Bu[13,23] (687 mg, 1.06 mmol) was dissolved in 5 mL of acetic anhydride under a N_2 atmosphere. Pd/C (10%, 70 mg) was carefully added and the reaction stirred at rt under a H_2 atmosphere until TLC indicated complete consumption of the starting material (overnight). The mixture was filtered through a pad of Celite and the filtrate concentrated under reduced pressure. Toluene (3 mL) was added and the mixture concentrated again to remove residual Ac_2O azeotropically. This process was repeated four times. No further purification was required: white solid; yield 573 mg, 97%; R_f 0.45 (CH_2Cl_2/MeOH, 95:5); mp = 235–237 °C; $[\alpha]^{25}_D$ = −26.8 (c = 1, MeOH); IR (ATR, cm^{-1}) 3311, 1652, 1532, 1147; ^{1}H NMR (300 MHz, CDCl3) δ_H 7.30 (s, 1H), 7.13 (s, 1H), 6.92 (s, 1H), 6.43 (s, 1H), 6.22 (d, J = 5.4 Hz, 1H), 3.69 (dd, J = 7.0, 5.6 Hz, 1H), 2.07 (m, J = 7.0 Hz, 1H), 2.05 (s, 3H), 1.47–1.38 (m, 33H), 1.03 (d, J = 7.0 Hz, 3H), 1.00 (d, J = 7.0 Hz, 3H); ^{13}C NMR (75 MHz, CDCl3) δ_C 174.3, 173.9, 173.5, 173.5, 172.1, 171.8, 80, 61, 57.3, 57.2, 56.9, 56.3, 28.1, 26.2, 25,2, 25.0–24.4 (overlapping signals), 23.2, 19.4, 19.3; HRMS (TOF ES$^+$, MeOH) calcd for $C_{27}H_{50}N_5O_7$ [M + 1]$^+$ 556.3702, found 556.3705.

*Ac-(αMe)Val-Aib$_4$OH (**4**).* The *tert*-butyl ester of **4** was prepared as described for peptide **3** starting from Cbz-L-(αMe)Val-Aib$_4$-O-*t*-Bu.[13] Ac-(αMe)Val-Aib$_4$-O-*t*-Bu was obtained as a white solid: yield 460 mg, 98%; R_f 0.55 (CH_2Cl_2/MeOH, 95:5); mp = 212–214 °C; $[\alpha]^{25}_D$ = +16.0 (c = 1, MeOH); IR (ATR, cm^{-1}) 3298, 1667, 1643, 1538, 1148; ^{1}H NMR (400 MHz, $CDCl_3$) δ_H 7.51 (s, 1H), 7.35 (s, 1H), 7.31 (s, 1H), 6.32 (s, 1H), 6.12 (s, 1H), 2.04 (s, 3H), 2.03 (m, J = 5.5 Hz, 1H), 1.47–1.39 (m, 36H), 0.97 (d, J = 5.0 Hz, 3H), 0.91 (d, J = 5.0 Hz, 3H); ^{13}C NMR (100 MHz, $CDCl_3$) δ_C 174.1, 174.0, 173.9, 173.8,

dx.doi.org/10.1021/jo302705k | J. Org. Chem. 2013, 78, 2248–2255

172.4, 171.2, 79.8, 62.9, 57.1, 56.9, 56.7, 56.1, 35.1, 27.9, 26.5, 26.3, 26.1, 25.2, 24.5−23.9, 17.2, 17.0; MS (ES$^+$, MeOH) m/z = ([M + Na]$^+$, 10%); HRMS (TOF ES$^+$, MeOH) calcd for $C_{28}H_{52}N_5O_7$ [M + 1]$^+$ = 570.3870, found 570.3862.

To a stirred solution of Ac-(αMe)Val-Aib$_4$-O-*t*-Bu (400 mg, 0.70 mmol) in distilled CH_2Cl_2 (3 mL) was added trifluoroacetic acid (3 mL) dropwise. The course of the reaction was followed by TLC. After reaction completion (4 h), the mixture was concentrated in vacuo. Et_2O was added to the residue (10 mL) and the solvent evaporated. This process was repeated five times. No further purification was required. Compound **4** was obtained as a white solid: yield 342 mg, 95%; R_f 0.35 (CH_2Cl_2/MeOH, 95:5); mp =273−275 °C; $[\alpha]^{25}_D$ = +19.2; IR (ATR, cm^{-1}) 3273, 3353, 1651, 1644, 1527, 1170; ^{1}H NMR (500 MHz, CD_3OD) δ_H 7.94 (brs, 1H), 7.93 (brs, 1H), 7.85 (brs, 1H), 7.69 (brs, 1H), 2.04 (s, 3H), 2.02 (m, J = 7.0 Hz, 1H), 1.51−1.38 (m, 27H), 1.00 (d, J = 7.0 Hz, 3H), 0.97 (d, J = 7.0 Hz, 3H); ^{13}C NMR (100 MHz, CD_3OD) δ_C 178.4, 176.9, 176. 8, 174.6, 174.5, 174.3, 62.0, 61.9, 58.1, 58.0, 58.0, 57.9, 57.2, 30.1, 27.0, 26.9, 26.8, 26.5, 25.9, 24.7−24.13 (overlapping signals), 22.5, 19.7; MS (ES$^+$, MeOH) m/z = ([M + Na]$^+$, 100); HRMS (TOF ES$^+$, MeOH) calcd for $C_{24}H_{44}N_5O_7$ [M + 1]$^+$ = 514.3236, found 514.3232.

X-ray Diffraction. Crystals suitable for X-ray analysis were obtained by slow evaporation from methanol for both peptides **3** and **4**. Crystals of peptide **3** are monoclinic, space group $P2_1$, with unit-cell dimensions a = 9.2540(14) Å, b = 17.036(3) Å, c = 10.3534(16) Å, and β = 94.202(3)° and those of peptide **4** are orthorhombic, with space group $P2_1$ and unit cell dimensions a = 11.926(2) Å, b = 8.7132(17) Å, and c = 13.814(3) Å, and β = 94.826(4). The crystal data, refinement details and structural parameters are summarized in Tables 1 and 2. Data collection for both peptide **3** and **4** was carried out on a CCD diffractometer with graphite-monochromated Mo Kα radiation, cryocooling to 100 K. The structures were solved by direct methods and refined by full-matrix least-squares against $F2$.[51]

In **3**, there is a water molecule in the asymmetric unit. All non-H atoms were refined anisotropically. H atoms bonded to C were included in calculated positions; those hydrogen atoms bonded to nitrogen and oxygen were found by difference Fourier methods and refined with U_{eq} values 1.2 (nitrogen) or 1.5 (oxygen) times that of the parent atom. The crystal data for **3** and **4** have been deposited with the Cambridge Crystallographic Data Centre, deposition nos. 907153 and 907154, respectively.

Nuclear Magnetic Resonance. Peptides **1** and **2** were dissolved in CD_3OH (peptide concentrations: 15 mM). All NMR experiments were performed on a Bruker Avance II+ 500 MHz spectrometer using the TOPSPIN 2.1 software package. Suppression of the alcohol OH signal was achieved using the WATERGATE pulse sequence. Phase sensitive DQF-COSY,[34] NOESY,[27,33] and TOCSY[26,27] were acquired by collecting 512, 480, and 400 increments, respectively, each one consisting of 16−40 scans and 16K data points. The spin-lock pulse for the TOCSY experiments was 70 ms long. To optimize the digital resolution in the carbon dimension, HMQC experiments[28] were acquired using a spectral width of 30 ppm centered at 22 ppm in F_1. The HMQC experiments were recorded with 200 t_1 increments, of 92 scans and 1K points each.[28] The nondecoupled HMQC experiment[29] used to measure $^1J_{C\alpha H\alpha}$ coupling constants was performed using a spectral width in F_1 of 150 ppm centered at 80 ppm, 512 t_1 experiments of 72 scans, and 16K points in F_2. All suitable, nonoverlapping cross-peaks of the NOESY spectrum of peptide **1** were integrated using the SPARKY 3.111 software package. Each interproton distance (d_i) was obtained from the corresponding cross-peak volume V_i applying the equation: $d_i = [(d_0 \cdot V_0)/V_i]^{1/6}$, where d_0 and V_0 are the calibration distance and volume. Distance calibration is usually based on the average of the integration values of the cross peaks due to interactions between β-geminal protons (e.g., CH_2 of glycines and/or of other amino acid residues) set to a distance of 1.8 Å. However, in peptide 1 the β-geminal protons of Gly^6 are very strongly coupled, and an important scalar contribution to their NOE cross-peaks could not be avoided at any of the mixing times tested. Another established way to calibrate distances when β-geminal protons are not available is the use of sequential distances [for instance, $d(H_i^\alpha, H_{i+1}N)$ or $d(H_iN, H_{i+1}N)$] in regular secondary structural elements.[52,53] This being the case for the amino acid sequence Aib^3-Gly^7 of peptide **1**, calibration was performed by calculating the average of cross-peak integration values due to interactions between amide protons of the above-mentioned peptide sequence (with the clear exclusion of Aib^5 HN−Aib^4 HN, completely overlapped by the diagonal peaks, see Figure 5) set to a distance of 2.80 Å. For all of the distances obtained, a standard deviation of ±10% was estimated.

■ ASSOCIATED CONTENT

Supporting Information

NMR spectra and X-ray data for **3** and **4**. Detailed data from NMR experiments on **1** and **2**. This material is available free of charge via the Internet at http://pubs.acs.org.

■ AUTHOR INFORMATION

Corresponding Author

*E-mail: clayden@man.ac.uk.

Notes

The authors declare no competing financial interest.

■ ACKNOWLEDGMENTS

We are grateful to the European Research Council (Advanced Grant ROCOCO) for funding this work. We thank Accademia dei Lincei of Rome for a fellowship (to M.D.Z.). We thank Prof. Claudio Toniolo and Prof. Fernando Formaggio for first suggesting to us the role of the N-terminal turn structure in governing screw-sense preference and for helpful comments on the manuscript.

■ REFERENCES

(1) Shamala, N.; Nagaraj, R.; Balaram, P. *J. Chem. Soc., Chem. Commun.* **1978**, 996−997.
(2) Benedetti, E.; Bavoso, A.; Di Blasio, B.; Pavone, V.; Pedone, C.; Crisma, M.; Bonora, G. M.; Toniolo, C. *J. Am. Chem. Soc.* **1982**, *104*, 2437−2444.
(3) Prasad, B. V. V; Balaram, P. *CRC Crit. Rev. Biochem.* **1984**, *16*, 307−348.
(4) Venkatraman, J.; Shankaramma, S. C.; Balaram, P. *Chem. Rev.* **2001**, *101*, 3131−3152.
(5) Toniolo, C.; Benedetti, E. *Trends Biochem. Sci.* **1991**, *16*, 350−353.
(6) Toniolo, C.; Crisma, M.; Formaggio, F.; Peggion, C. *Biopolymers (Pept. Sci.)* **2001**, *60*, 396−419.
(7) Hummel, R. P.; Toniolo, C.; Jung, G. *Angew. Chem., Int. Ed. Engl.* **1987**, *99*, 1180.
(8) Kubasik, M. A.; Kotz, J.; Szabo, C.; Furlong, T.; Stace, J. *Biopolymers* **2005**, *78*, 87−95.
(9) Kubasik, M.; Blom, A. *ChemBioChem* **2005**, *6*, 1187−1190.
(10) Clayden, J.; Castellanos, A.; Solà, J.; Morris, G. A. *Angew. Chem., Int. Ed.* **2009**, *48*, 5962−5965.
(11) Inai, Y.; Tagawa, K.; Takasu, A.; Hirabayashi, T.; Oshikawa, T.; Yamashita, M. *J. Am. Chem. Soc.* **2000**, *122*, 11731−11732.
(12) Solà, J.; Morris, G. A.; Clayden, J. *J. Am. Chem. Soc.* **2011**, *133*, 3712−3715.
(13) Brown, R. A.; Marcelli, T.; De Poli, M.; Solà, J.; Clayden, J. *Angew. Chem., Int. Ed.* **2012**, *51*, 1395−1399.
(14) Brändén, C.-I.; Tooze, J. In *Introduction to Protein Structure*; Garland Publisher: New York, 1999.
(15) Dunitz, J. D. *Angew. Chem., Int. Ed.* **2001**, *40*, 4167−4173.
(16) Venkatachalam, C. *M. Biopolymers* **1968**, *6*, 1425−1436.
(17) Inai, Y.; Kurokawa, Y.; Hirabayashi, T. *Biopolymers* **1999**, *49*, 551−564.
(18) Benedetti, S.; Saviano, M.; Iacovino, R.; Crisma, M.; Formaggio, F.; Toniolo, C. *Z. Kristallogr.* **1999**, *214*, 160−166.

(19) Ramachandran, G. N.; Ramakrishnan, C.; Sasisekharan, V. *J. Mol. Biol.* **1963**, *7*, 95−99.
(20) Ramakrishnan, C.; Ramachandran, G. N. *Biophys. J.* **1965**, *5*, 909−932.
(21) Zimmerman, S. S.; Pottle, M. S.; Némethy, G.; Scheraga, H. A. *Macromolecules* **1977**, *10*, 1−9.
(22) Toniolo, C.; Valle, G.; Bonora, G. M.; Crisma, M.; Formaggio, F.; Bavoso, A.; Benedetti, E.; Di Blasio, B.; Pavone, V.; Pedone, C. *Biopolymers* **1986**, *25*, 2237−2253.
(23) Pengo, B.; Formaggio, F.; Crisma, M.; Toniolo, C.; Bonora, G. M.; Broxterman, Q. B.; Kamphius, J.; Saviano, M.; Iacovino, R.; Rossi, F.; Benedetti, E. *J. Chem. Soc., Perkin Trans. 2* **1998**, 1651−1657.
(24) Datta, S.; Shamala, N.; Banerjee, A.; Pramanik, A.; Bhattacharjya, S.; Balaram, P. *J. Am. Chem. Soc.* **1997**, *119*, 9246−9251.
(25) Wüthrich, K. In *NMR of Proteins and Nucleic Acids*; Wiley: New York, 1986.
(26) Bax, A.; Davis, D. G. *J. Magn. Reson.* **1985**, *65*, 355−360.
(27) Piotto, M.; Saudek, V.; Sklenar, V. *J. Biomol. NMR* **1992**, *2*, 661−666.
(28) Bax, A.; Subramanian, S. *J. Magn. Reson.* **1986**, *67*, 565−569.
(29) Bax, A.; Griffey, R. H.; Hawkins, B. L. *J. Magn. Reson.* **1983**, *55*, 301−315.
(30) Jung, G.; Brückner, H.; Bosch, R.; Winter, W.; Schaal, H.; Strähle, J. *Liebigs Ann. Chem.* **1983**, 1096−1106.
(31) Anders, R.; Wenschuh, H.; Soskic, V.; Fischer-Frühholz, S.; Ohlenschläger, O.; Dornberger, K.; Brown, L. R. *J. Peptide Res.* **1998**, *52*, 34−44.
(32) Bellanda, M.; Peggion, E.; Bürgi, R.; van Gunsteren, W.; Mammi, S. *J. Pept. Res.* **2001**, *57*, 97−106.
(33) Sklenar, V.; Piotto, M.; Leppik, R.; Saudek, V. *J. Magn. Reson. Ser. A* **1993**, *102*, 241−245.
(34) Rance, M.; Sørensen, O. W.; Bodenhausen, G.; Wagner, G.; Ernst, R. R.; Wüthrich, K. *Biochem. Biophys. Res. Commun.* **1983**, *117*, 479−485.
(35) Vuister, G. W.; Delaglio, F.; Bax, A. *J. Am. Chem. Soc.* **1992**, *114*, 9674−9675.
(36) Lam, S. L.; Hsu, V. L. *Biopolymers* **2003**, *69*, 270−281.
(37) Pardi, A.; Billeter, M.; Wüthrich, K. *J. Mol. Biol.* **1984**, *180*, 741−751.
(38) Hovmöller, S.; Zhou, T.; Ohlson, T. *Acta Crystallogr. D* **2002**, *58*, 768−776.
(39) Bonora, G. M.; Mapelli, C.; Toniolo, C.; Wilkening, R. R.; Stevens, E. S. *Int. J. Biol. Macromol.* **1984**, *6*, 179−188.
(40) Augspurger, J. D.; Bindra, V. A.; Scheraga, H. A.; Kuki, A. *Biochemistry* **1995**, *34*, 2566−2576.
(41) Wipf, P.; Kunz, R. W.; Prewo, R.; Heimgartner, H. *Helv. Chim. Acta* **1998**, *71*, 268−278.
(42) Polese, A.; Formaggio, F.; Crisma, M.; Valle, G.; Toniolo, C.; Bonora, G. M.; Broxterman, Q. B.; Kamphuis, J. *Chem.—Eur. J.* **1996**, *2*, 1104−1111.
(43) Inai, Y.; Kurokawa, Y.; Kojima, N. *J. Chem. Soc., Perkin Trans. 2* **2002**, 1850−1857.
(44) Inai, Y.; Ishida, Y.; Tagawa, K.; Takasu, A.; Hirabayashi, T. *J. Am. Chem. Soc.* **2002**, *124*, 2466−2473.
(45) Pace, C. N.; Scholtz, J. M. *Biophys. J.* **1998**, *75*, 422−427.
(46) Blont, E. R. In *Polyamino Acids, Polypeptides, and Proteins*; Stahmann, A., Ed.; The University of Wisconsin Press: Madison, WI, 1962; pp 275−279.
(47) Minor, D. L.; Kim, P. S. *Nature* **1994**, *367*, 660−663.
(48) Baron, M. H.; De Lozé, C.; Toniolo, C.; Fasman, G. D. *Biopolymers* **1979**, *18*, 411−424.
(49) Published crystal structures of related compounds reveal L-Val and L-Phe participating in right-handed type III turns and in left-handed type III′ turns in the solid state. See: (a) Reference 50. (b) Solà, J.; Helliwell, M.; Clayden, J. *J. Am. Chem. Soc.* **2010**, *132*, 4548−4549. (c) Boddaert, T.; Clayden, J. *Chem. Commun.* **2012**, *48*, 3397−3399.
(50) The left-handed screw sense in crystal structures of Aib oligomers carrying N-terminal L-amino acids had previously been ascribed to crystal packing forces: Solà, J.; Helliwell, M.; Clayden, J. *Biopolymers* **2011**, *95*, 62−65.
(51) Sheldrick, G. M. *Acta Crystallogr. A* **2008**, *64*, 112.
(52) Billeter, M.; Braun, W.; Wüthrich, K. *J. Mol. Biol.* **1982**, *155*, 321−346.
(53) Williamson, M. P.; Havel, T. F.; Wüthrich, K. *J. Mol. Biol.* **1985**, *182*, 295−315.